



RESEARCH ARTICLE

RNA-binding protein YBX1 promotes brown adipogenesis and thermogenesis via PINK1/PRKN-mediated mitophagy

Ruifan Wu¹  | Shuting Cao² | Fan Li¹ | Shengchun Feng¹ | Gang Shu¹ | Lina Wang¹ | Ping Gao¹ | Xiaotong Zhu¹ | Canjun Zhu¹ | Songbo Wang¹  | Qingyan Jiang¹

¹Guangdong Laboratory of Lingnan Modern Agriculture, Guangdong Province Key Laboratory of Animal Nutritional Regulation and National Engineering Research Center for Breeding Swine Industry, College of Animal Science, South China Agricultural University, Guangzhou, China

²State Key Laboratory of Livestock and Poultry Breeding, Ministry of Agriculture Key Laboratory of Animal Nutrition and Feed Science in South China, Guangdong Key Laboratory of Animal Breeding and Nutrition, Maoming Branch, Guangdong Laboratory for Lingnan Modern Agriculture, Institute of Animal Science, Guangdong Academy of Agricultural Sciences, Guangzhou, China

Correspondence

Qingyan Jiang, Guangdong Laboratory of Lingnan Modern Agriculture, Guangdong Province Key Laboratory of Animal Nutritional Regulation and National Engineering Research Center for Breeding Swine Industry, College of Animal Science, South China Agricultural University, Guangzhou 510642, China.

Email: qyjiang@scau.edu.cn

Funding information

National Natural Science Foundation of China, Grant/Award Number: 31790411 and 31972636; China Postdoctoral Science Foundation, Grant/Award Number: 2021M691073; Guangdong Basic and Applied Basic Research Foundation, Grant/Award Number: 2021A1515111085

Abstract

Promoting the thermogenic function of brown adipose tissue (BAT) is a promising strategy to combat obesity and metabolic disorders. While much is known about the transcriptional regulation of BAT activation, however, the underlying mechanism of post-transcriptional control by RNA binding proteins remains largely unknown. Here, we found that RNA binding protein Y-box binding protein 1 (YBX1) expression was abundant in BAT and induced by cold exposure and a β -adrenergic agonist in mice. Loss-of-function experiments showed that YBX1 deficiency inhibited mouse primary brown adipocyte differentiation and thermogenic function. Further study showed that YBX1 positively regulates thermogenesis through enhancing mitophagy. Mechanistically, RNA immunoprecipitation identified that YBX1 directly targeted the transcripts of PTEN-induced kinase 1 (*Pink1*) and parkin RBR E3 ubiquitin-protein ligase (*Prkn*), two key regulators of mitophagy. RNA decay assay proved that loss of YBX1 decreased mRNA stability of *Pink1* and *Prkn*, leading to reduced protein expression, thereby alleviating mitophagy and inhibiting thermogenic program. Importantly, in vivo experiments demonstrated that YBX1 overexpression in BAT promoted thermogenesis

Abbreviations: 3-MA, 3-methyladenine; Adipoq, adiponectin; BAT, brown adipose tissue; BNIP3, BCL2 interacting protein 3; CDS, coding sequence; Cox2, cytochrome c oxidase subunit 2; CSD, conserved cold shock domain; DRP1, dynamin related protein 1; EGFP, enhanced green fluorescent protein; FUNDC1, FUN14 domain containing 1; HFD, high-fat diet; JMD1C, jumonji domain containing 1C; MAP1LC3B/LC3, microtubule-associated protein 1 light chain 3 beta; mtDNA, mitochondrial DNA; Nrf1, nuclear respiratory factor 1; OCR, oxygen consumption rate; PINK1, PTEN-induced kinase 1; PPARG, peroxisome proliferator activated receptor gamma; PPARGC1A, proliferator-activated receptor gamma coactivator 1; PRDM16, PR domain-containing protein 16; PRKN, parkin RBR E3 ubiquitin protein ligase; qPCR, quantitative real-time PCR; RBPs, RNA-binding proteins; RIP, RNA-immunoprecipitation; siRNA, small interfering RNA; SQSTM1/p62, sequestosome-1; SVF, stromal-vascular fraction; T3, triiodothyronine; TFAM, transcription factor A, mitochondrial; UCP1, uncoupling protein1; WAT, white adipose tissue; YBX1, Y-box binding protein 1.

Ruifan Wu and Shuting Cao contributed equally to this work.

and mitophagy in mice. Collectively, our results reveal novel insight into the molecular mechanism of YBX1 in post-transcriptional regulation of PINK1/PRKN-mediated mitophagy and highlight the critical role of YBX1 in brown adipogenesis and thermogenesis.

KEYWORDS

adipogenesis, mitophagy, PINK1/PRKN, thermogenesis, YBX1

1 | INTRODUCTION

The global rise in obesity and its associated metabolic diseases has precipitated the need for novel approaches to reduce adiposity. Obesity is caused by an imbalance in which energy intake exceeds energy expenditure.¹ White adipose tissue (WAT) stores triglyceride as chemical energy, while brown adipose tissue (BAT) dissipates the chemical energy to generate heat through mitochondrial uncoupling protein1 (UCP1) and can oppose obesity and improve glucose and lipid homeostasis in humans and mice.^{2–4} Thus, the identification of targetable factors that promote the differentiation and function of brown adipocytes is a potential way to treat obesity.

Recent data have shown that selective autophagy of mitochondria, known as mitophagy, plays an essential role in the physiology of the mitochondria-enriched brown adipocytes and energy metabolism.⁵ Mitophagy is driven by specific proteins, including PTEN-induced kinase 1 (PINK1), parkin RBR E3 ubiquitin-protein ligase (PRKN), BCL2 interacting protein 3 (BNIP3), and FUN14 domain containing 1 (FUNDC1), interacting with autophagosomal protein microtubule-associated protein 1 light chain 3 beta (MAP1LC3B) that drives autophagosomes and degrades its contents.⁶ PINK1 is a core regulator of mitophagy, which activates the E3 ubiquitin ligase PRKN to mark depolarized mitochondria for degradation. Cold exposure at 4°C induces mitophagy in BAT, suggesting that mitophagy is needed for adaptive thermogenesis.⁷ Recently, studies showed that mitophagy deficiency-induced brown fat dysfunction and aggravated obesity in mice.^{8,9} Thyroid hormone triiodothyronine (T3) was reported to stimulate BAT activation and thermogenesis via promoting mitochondrial autophagy, activity, and lipid metabolism in BAT, which have potential beneficial effects on obesity.¹⁰ Therefore, it is significant to investigate the mechanisms underlying the regulation of mitophagy and the thermogenic function of brown adipocytes.

Previous studies have mainly focused on transcriptional control of molecular pathways that mediate BAT activation.¹¹ By contrast, post-transcriptional regulation of thermogenesis by RNA-binding proteins (RBPs) is largely

unexplored. Emerging evidence suggests that RBPs lie at the center of post-transcriptional regulation by governing the fate of mRNA transcripts from biogenesis, splicing, stabilization, and translation to RNA decay.^{12,13} The Y-box binding protein 1 (YBX1) is a member of the family of DNA- and RNA-binding proteins with an evolutionarily ancient and conserved cold shock domain (CSD).¹⁴ Proteins bearing CSDs have been reported to regulate cellular adaptation response to cold stress mainly at post-transcriptional levels.¹⁵ Thus, the presence of CSD suggests that YBX1 may play a role in BAT thermogenesis. A recent study found that YBX1 knockdown inhibited white preadipocytes commit to beige lineage and impaired thermogenic potential partially through mediating histone demethylase jumonji domain containing 1C (JMJD1C) at the transcriptional level.¹⁶ However, the post-transcriptional regulation of YBX1 in thermogenesis of brown fat cells and its function under physiologic conditions in vivo remains unclear.

In this study, we investigated the post-transcriptional control by RNA binding protein YBX1 in brown adipocyte activation and the underlying network between thermogenesis and mitophagy. We revealed that YBX1 promoted brown adipocyte differentiation and thermogenic function through enhancing PINK1/PRKN-mediating mitophagy. Overexpression of YBX1 in BAT promoted thermogenesis and mitophagy in mice. Our findings unveil a new role for YBX1 as a positive regulator of mitophagy and provide a novel insight into the molecular mechanism of YBX1 in the regulation of brown adipogenesis and thermogenesis.

2 | MATERIALS AND METHODS

2.1 | Animals

C57BL/6 mice were housed under the controlled room temperature (22°C ± 2°C) with 12 h light and dark cycles and free access to water and food. For the CL316,243 treatment experiment, the mice were injected intraperitoneally with CL316,243 at a dose of 1 mg/kg for 7 days. The mice were sacrificed and subcutaneous WATs and interscapular BAT were collected. All animal experiments were

carried out according to the guidelines of The Animal Ethics Committee of South China Agricultural University.

2.2 | Cold exposure experiment

For acute cold exposure experiment, mice were individually housed and placed in a freezer (4°C) for 6 h with free access to food and water. After cold exposure, mice were sacrificed, subcutaneous WATs and interscapular BAT were collected for protein and gene analysis. Core body temperature was measured using a microprobe thermometer.

2.3 | Cell culture and brown adipocyte differentiation

Isolation of primary brown preadipocytes from BAT and induction of adipocyte differentiation were performed as previously reported.¹⁰ Briefly, the interscapular BAT was excised from 3-week-old C57BL/6 mice, minced, and then digested with 1 mg/ml type I collagenase (Gibco) at 37°C for 30 min. After filtering through a 70 µm cell strainer, the pellet containing preadipocytes was centrifuged at 500 g for 5 min. Preadipocytes were maintained in DMEM supplemented with 10% fetal bovine serum (FBS; Gibco), 1% penicillin-streptomycin at 37°C in a 5% CO₂ humidified incubator. Cells were tested negative for mycoplasma contamination before use. For adipocyte differentiation, post-confluent primary brown preadipocytes were induced by induction medium containing 0.5 mM IBMX, 1 µM dexamethasone, 5 µg/ml insulin, 1 nM T3, 125 nM indomethacin, and 10% FBS for 2 days. The cells were then switched to a maintenance medium containing 10% FBS, 5 µg/ml insulin, and 1 nM T3 for 6 more days. Mdivi-1 and 3-MA (MedChemExpress) were used to treated cells to inhibit autophagy/mitophagy.

2.4 | Cell transfection and virus infection

The small interfering RNA (siRNA) transfection was performed using Lipofectamine 2000 (Invitrogen) according to the manufacturers' instructions. The sequence for negative control siRNA is as follows (5' to 3'): 5'-UUCUCCGAACGUGUCACGUTT-3'. Mouse *Ybx1* siRNA #1 and #2 were ordered from Genescript which targets 5'-GUCAAAUGGUUCAAUGUAA-3' and 5'-GGAGGCAGCAAUGUUACA-3', respectively. Mouse *Pink1* siRNA targets 5'-GGGAUCUCAAGUCC GACAACA-3', while *Prkn* siRNA targets 5'-AUUCCAAAC CGGAUGAGUGGU-3. The YBX1- and enhanced green fluorescent protein (EGFP)-expressing adenovirus were

generated from Hanbio. For adenoviral infection of primary brown preadipocytes, 50% of confluent cell cultures were incubated with adenovirus in a growth medium for 48 h, followed by replacement with fresh growth medium. For adenoviral infection of BAT, mice were anesthetized using isoflurane. The BAT was surgically exposed and injected with adenovirus. The incision was closed, and animals were allowed to recover. After 1 week, the mice were killed and BAT were subjected to examine the efficiency of adenovirus.

2.5 | Western blot assay

Cells and tissue were lysed in RIPA buffer supplemented with protease and phosphatase inhibitor cocktail. The protein concentration was detected using a BCA assay kit (Thermo Fisher Scientific). Protein samples were separated by SDS-PAGE and transferred to PVDF Membrane (Millipore). The membrane was blocked with non-fat milk and then incubated with relevant primary antibodies at 4°C overnight, followed by an HRP-conjugated secondary antibody. Immunoreactive proteins in the membrane were scanned using a FluorChem M Fluorescent Imaging System (ProteinSimple). The relative protein expression was performed using the ImageJ software and the band density was normalized to ACTB expression. Primary antibodies information was listed in Table S1.

2.6 | RNA extraction and quantitative real-time PCR (qPCR) analysis

The total RNAs from tissue or cells were purified using TRIzol Reagent (Invitrogen) and converted to cDNA with M-MLV reverse transcriptase (Promega). Quantitative real-time PCR (qPCR) analysis was performed using SYBR Green PCR Master Mix (Roche) following the manufacturer's instructions and analyzed with Applied Biosystems QuantStudio 3 Real-Time PCR System (Thermo Fisher Scientific). Results were normalized to *Actb*. The primer sequences were listed in Table S2.

2.7 | Measurement of mitochondrial DNA (mtDNA)

The total DNA was isolated from primary brown adipocytes with DNAzol reagent (Invitrogen) according to the manufacturer's instructions. mtDNA was amplified using primers specific for the mitochondrial cytochrome c oxidase subunit 2 (*Cox2*) gene and normalized to an intron of the nuclear-encoded *Hbb* (β-globin) gene as described before.¹⁷ The primer sequences were listed in Table S2.

2.8 | Immunofluorescence assay

For immunofluorescence assay, cells were fixed with 4% paraformaldehyde, permeabilized by 0.1% Triton X-100, and incubated with YBX1 or UCP1 primary antibodies overnight, followed by secondary antibody conjugated with FITC or Cy3 for 1 h and DAPI staining for 10 min. For examining the colocalization of mitochondria and autophagosome, cells were incubated with MitoTracker (Invitrogen) for 30 min, then stained with MAP1LC3B and DAPI. For staining of BAT sections, BAT samples were rapidly frozen using liquid nitrogen and fixed in Tissue-Tek OCT. Then, we sliced BAT into 10 μ m by a cryostat (CM1850, Leica) for staining. Immunofluorescent

samples were imaged by a confocal laser microscope (Carl Zeiss Ltd).

2.9 | RNA immunoprecipitation-qPCR (RIP-qPCR)

RIP-qPCR analysis was adapted from the previous report.¹⁸ Briefly, FLAG-YBX1-overexpressing cells pellets were lysed in lysis buffer (150 mM KCl, 10 mM HEPES, 2 mM EDTA, 0.5% NP-40, 0.5 mM DTT, 1:100 protease inhibitor cocktail and RNase inhibitor) for 30 min at 4°C. The lysates were centrifuged, and the supernatant was transferred to pass through a 0.22 μ m membrane syringe. A small aliquot

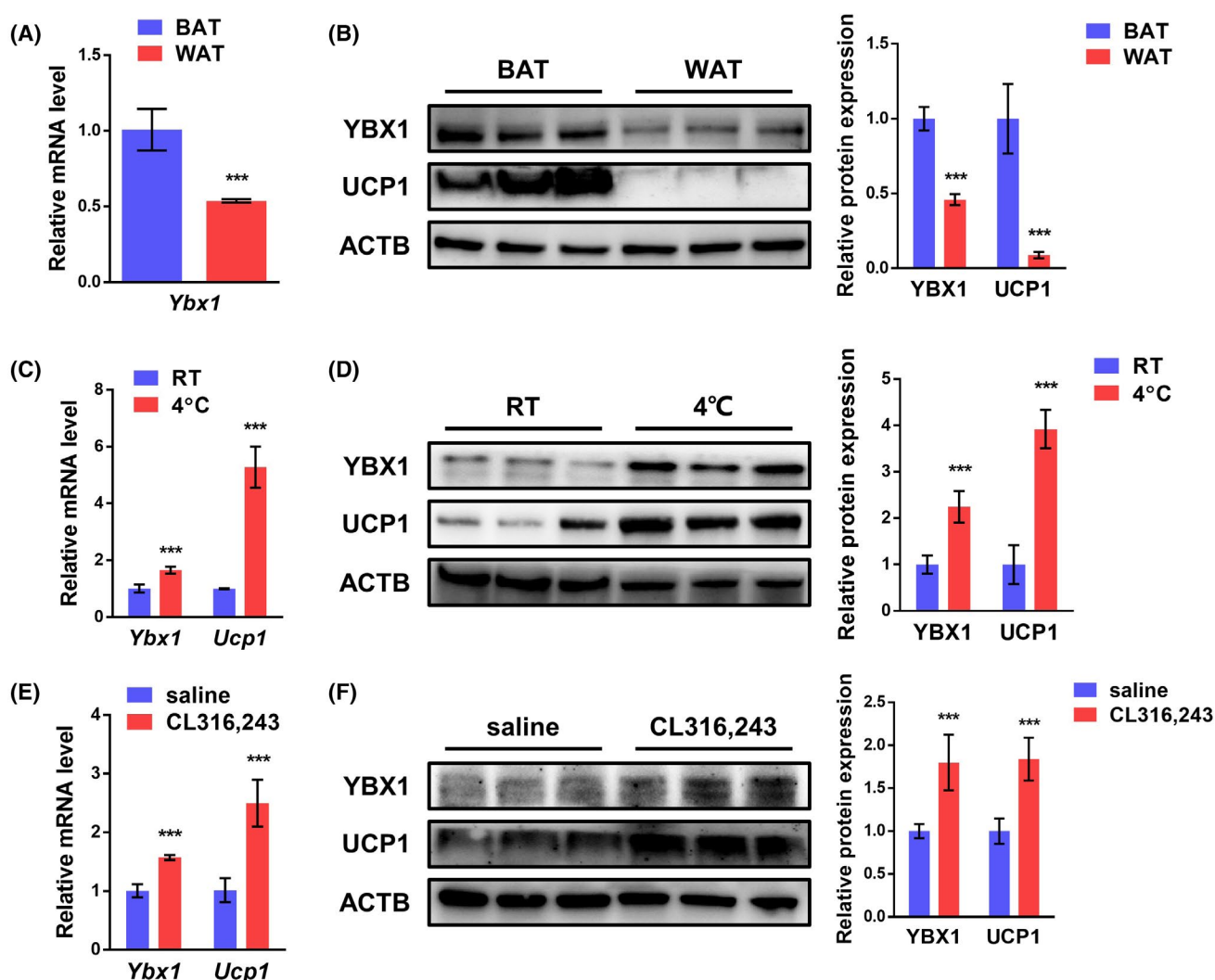


FIGURE 1 YBX1 is highly expressed in BAT and induced by cold exposure and β -adrenergic agonist. (A) Real-time quantitative PCR (qPCR) analysis of mRNA expression of *Ybx1* in BAT and WAT from 8-week-old male mice. (B) Western blot analysis of protein expression of YBX1 and UCP1 in BAT and WAT from 8-week-old male mice. (C) qPCR analysis of mRNA expression of *Ybx1* in BAT from mice with or without cold exposure (4°C) for 8 h. (D) Western blot analysis of protein expression of YBX1 and UCP1 in BAT from mice with or without cold exposure (4°C) for 8 h. (E) qPCR analysis of mRNA expression of *Ybx1* in BAT from mice injected daily with or without CL316,243 at 1 mg/kg for 7 days. (F) Western blot analysis of protein expression of YBX1 and UCP1 in BAT from mice injected daily with or without CL316,243 at 1 mg/kg for 7 days. The data were presented as the mean \pm SD ($n = 6$). *** $p < .001$

of the lysate was saved as input, and the remaining sample was incubated with anti-FLAG or IgG magnetic beads (Beyotime Biotechnology) for 4 h at 4°C. Then, the beads were eluted in a wash buffer containing 3 × FLAG peptide. The input and immunoprecipitated RNAs were isolated by TRIzol and were reverse transcribed into cDNA. The fold enrichment was detected by qPCR.

2.10 | Transmission electron microscopy

The cells were washed with PBS and fixed in 2.5% glutaraldehyde in phosphate buffer (0.1 M, pH 7.0) for 4 h and post-fixed with 1% OsO₄ in phosphate buffer (0.1 M, pH 7.0) for 2 h. Cell pellets were dehydrated with an acetone series and embedded in epoxy resin. Ultra-thin sections were cut and double-stained with uranyl acetate

and lead citrate. Images were taken using JEM-2010 HR transmission electron microscopy (JEOL).

2.11 | mRNA decay assay

NC and YBX1 knockdown cells were treated with 5 µg/ml actinomycin D to inhibit mRNA transcription. Samples were collected at the indicated time points. The total RNA was extracted and the mRNA levels of interest were analyzed by qPCR. *Actb* was used as an internal control.

2.12 | Oxygen consumption rate analysis

The mitochondrial oxygen consumption rate (OCR) of brown adipocytes was measured using a Seahorse XF96

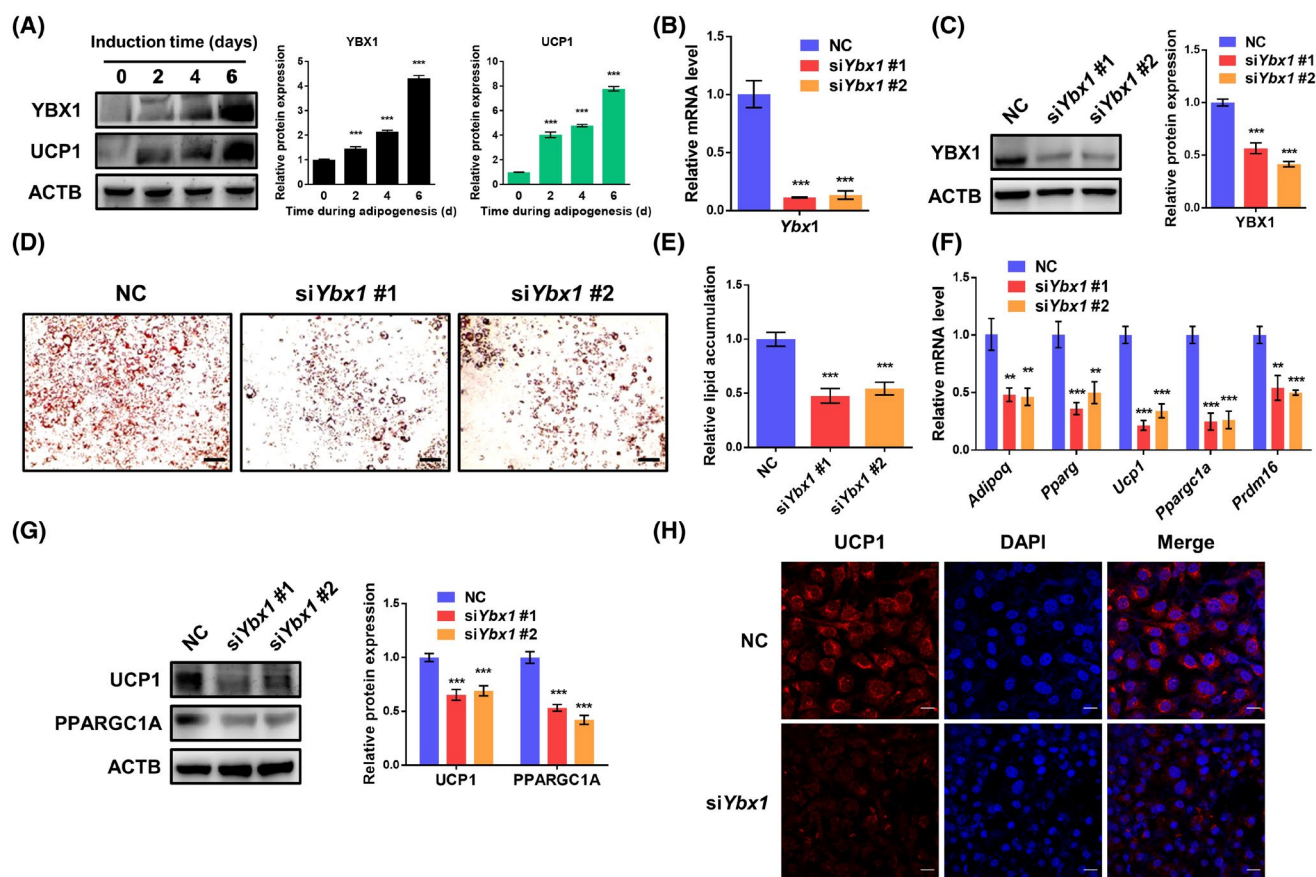
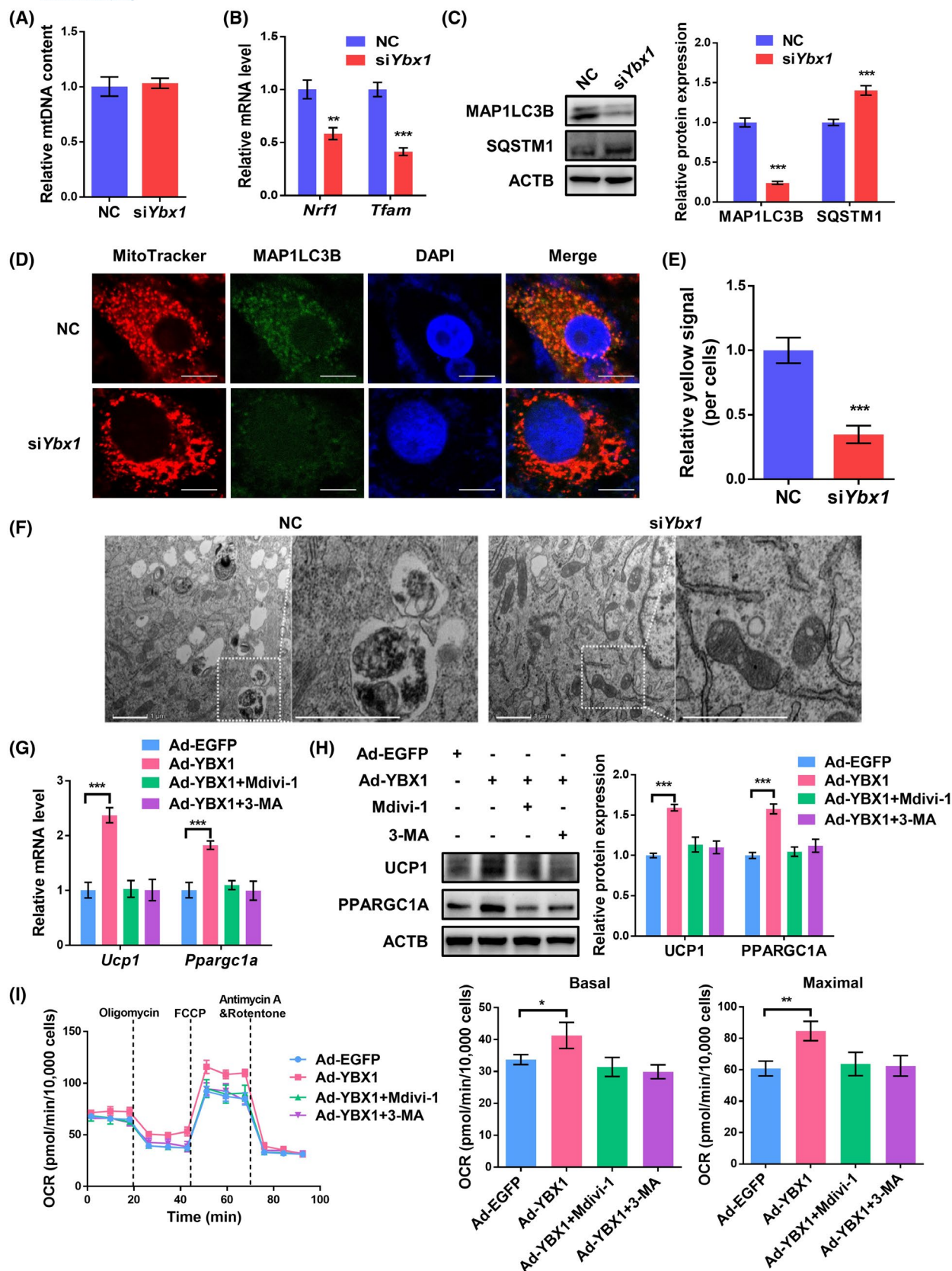


FIGURE 2 Knockdown of YBX1 inhibits brown adipogenesis and thermogenesis. (A) Western blot analysis of protein expression of YBX1 and UCP1 during mouse primary brown adipogenesis. (B) qPCR analysis of YBX1 knockdown efficiency in primary brown preadipocytes treated with negative control (NC) or *Ybx1* siRNAs. (C) Western blot analysis of YBX1 knockdown efficiency in primary brown preadipocytes treated with NC or *Ybx1* siRNAs. (D) Oil Red O staining of differentiated brown preadipocytes treated with NC or *Ybx1* siRNAs. Scale bar: 100 µm. (E) Relative lipid accumulation was quantified with a microplate spectrophotometer at 500 nm. (F) qPCR analysis of mRNA expression of *Adipoq*, *Pparg*, *Ucp1*, *Ppargc1a*, and *Prdm16* in differentiated brown preadipocytes treated with NC or *Ybx1* siRNAs. (G) Western blot analysis of protein expression of UCP1 and PPARGC1A in differentiated brown preadipocytes treated with NC or *Ybx1* siRNAs. (H) Immunofluorescent staining of UCP1 in differentiated brown preadipocytes treated with NC or *Ybx1* siRNA. Scale bar, 20 µm. The data were presented as the mean ± SD from three independent experiments. ***p* < .01, ****p* < .001



Extracellular Flux Analyzer according to the manufacturer's instructions. Fully differentiated cells seeded on XF96 plate were subjected to a temperature-controlled (37°C) extracellular analyzer. After measuring the initial OCR,

1 μ M oligomycin, 2 mM FCCP, and 0.5 mM rotenone/ac-tinomycin A were then sequentially added into the plate by automatic pneumatic injection. After the assay, cells were trypsinized and total cell numbers from each well

were counted for normalization. Basal respiration was calculated as $[\text{OCR}_{\text{initial}} - \text{OCR}_{\text{R+A}}]$. Maximum respiration rate was computed as $[\text{OCR}_{\text{FCCP}} - \text{OCR}_{\text{R+A}}]$. Data were analyzed by Seahorse Wave software.

2.13 | Statistical analysis

All data were presented as the mean \pm SD from three independent experiments. All statistical tests were performed using GraphPad Prism 6 software. Statistical significance was assessed using a two-tailed Student's *t*-test (for comparison of two groups) or one-way ANOVA followed by a Tukey test (for comparison of three or more groups). Significance was established at $*p < .05$, $**p < .01$ or $***p < .001$.

3 | RESULTS

3.1 | YBX1 expression in BAT is upregulated by cold exposure and β -adrenergic agonist

To investigate the potential role of YBX1 in adipose tissue, we first detected its expression levels in different fat depots of mice. As shown in Figure 1A, the mRNA levels of *Ybx1* were higher in interscapular BAT than in subcutaneous WAT. Consistently, YBX1 protein abundance was also enriched in BAT (Figure 1B), suggesting the potential involvement of YBX1 in regulating thermogenesis. Since cold exposure and β -adrenergic agonists are two classical inducers of adaptive thermogenesis, we measured YBX1 expression in BAT from mice following cold exposure or β -adrenergic agonists CL316,243. As expected, UCP1 mRNA and protein levels in BAT were induced after cold exposure or CL316,243 treatment of mice (Figure 1C–F). Similarly, the expression of YBX1 was also significantly promoted by cold exposure or CL316,243 (Figure 1C–F). These results suggest that the induction of

YBX1 is required for the remodeling of thermogenic adipose tissues.

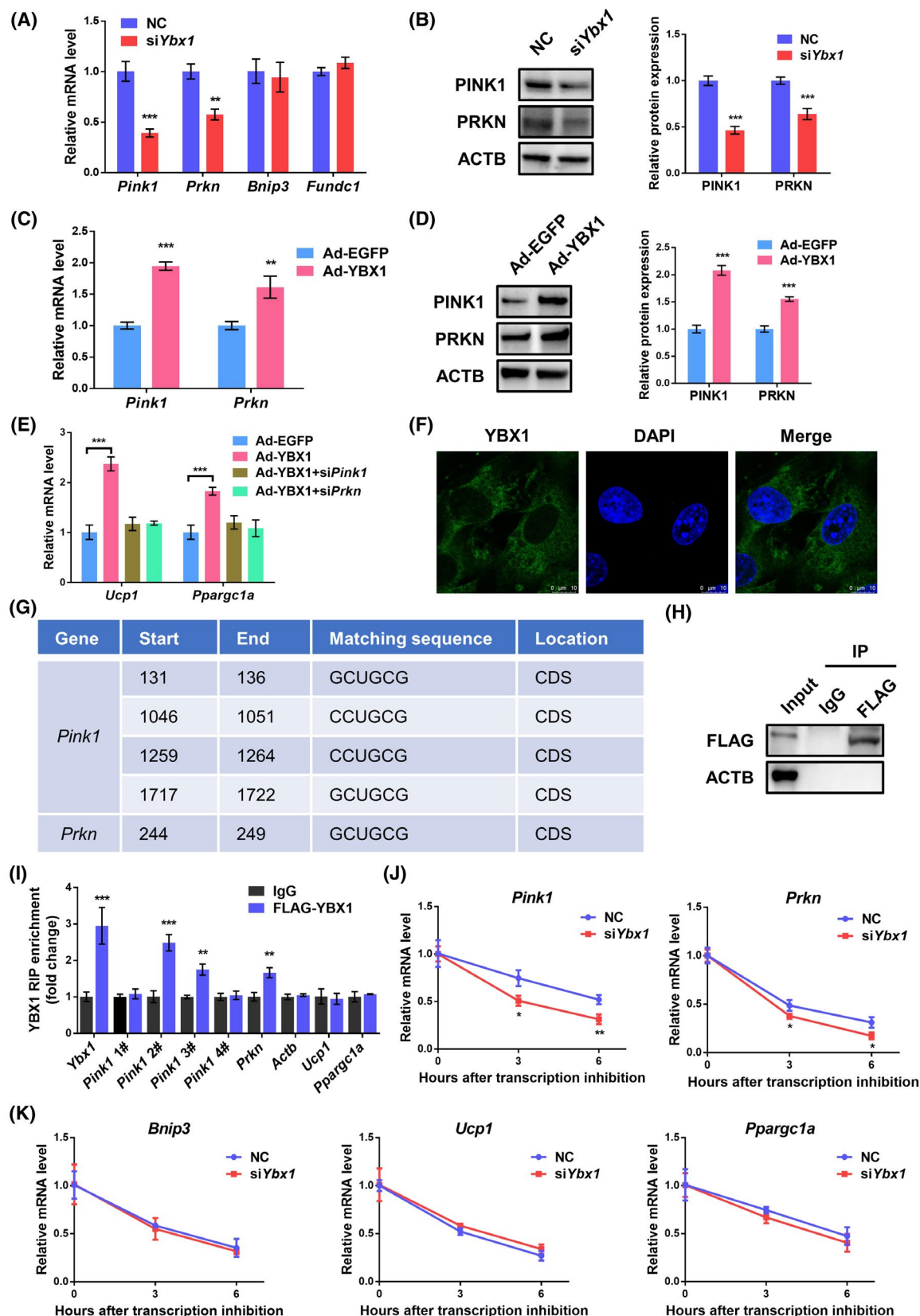
3.2 | YBX1 deficiency suppresses brown adipocyte differentiation and thermogenic gene expression

To investigate whether YBX1 influences brown adipocyte differentiation and thermogenesis, we isolated brown primary preadipocytes from mice and performed an in vitro brown adipogenesis assay. As shown in Figure 2A, both YBX1 and UCP1 were upregulated during brown adipocyte differentiation. Next, we performed YBX1 loss-of-function experiments using siRNA that exhibited about 45%–60% knockdown of endogenous YBX1 protein expression in cells (Figure 2B,C). Oil red O staining showed that loss of YBX1 severely inhibited brown adipogenesis and lipid accumulation (Figure 2D,E). In addition, YBX1 knockdown reduced the expression of general adipogenesis marker, such as adiponectin (*Adipoq*) and peroxisome proliferator-activated receptor gamma (*Pparg*) (Figure 2F). Importantly, YBX1 deficiency significantly decreased the mRNA and protein expression of thermogenic genes, including *Ucp1*, proliferator-activated receptor gamma co-activator 1 (*Ppargc1a*), and PR domain-containing protein 16 (*Prdm16*) (Figure 2F,G). Furthermore, immunofluorescence assay revealed a decreased UCP1 expression in YBX1-deficient brown adipocytes (Figure 2H). Collectively, these data indicate that YBX1 knockdown inhibits brown adipogenesis and thermogenic gene expression.

3.3 | YBX1 is essential for the thermogenic function of brown adipocytes by promoting mitophagy

Given the vital role of the mitochondria in the thermogenic capacity of brown adipocytes, we investigate whether YBX1 influences mitochondrial content and function.

FIGURE 3 YBX1 increases thermogenic gene expression in brown adipocytes via promoting mitophagy. (A) The relative mtDNA copy number in differentiated brown preadipocytes treated with NC or *Ybx1* siRNA. (B) qPCR analysis of mRNA expression of *Nrf1* and *Tfam* in differentiated brown preadipocytes treated with NC or *Ybx1* siRNA. (C) Western blot analysis of protein expression of MAP1LC3B and SQSTM1 in differentiated brown preadipocytes treated with NC or *Ybx1* siRNA. (D) Immunofluorescent staining of differentiated brown preadipocytes treated with NC or *Ybx1* siRNA. Red color represents mitochondria stained with MitoTracker Red. Green color represents MAP1LC3B. Yellow color represents the colocalization of mitochondria and autophagosome. Scale bar, 10 μm . (E) Quantitative analysis of the yellow fluorescence signal per cell. (F) Transmission electron microscopy analysis of autophagosomes in differentiated brown preadipocytes treated with NC or *Ybx1* siRNA. Scale bar: 1 μm . (G) qPCR analysis of mRNA expression of *Ucp1* and *Ppargc1a* in EGFP or YBX1-overexpressing brown adipocytes treated with or without 50 μM Mdivi-1 or 10 mM 3-MA. (H) Western blot analysis of MAP1LC3B, UCP1, and PPARGC1A in EGFP or YBX1-overexpressing brown adipocytes treated with or without 50 μM Mdivi-1 or 10 mM 3-MA. (I) Seahorse analysis of oxygen consumption rates (OCR) in EGFP or YBX1-overexpressing brown adipocytes treated with or without 50 μM Mdivi-1 or 10 mM 3-MA. $*p < .05$, $**p < .01$, $***p < .001$, Ad-YBX1 group compared to Ad-EGFP group. The basal and maximal OCR are shown in the right panel. The data were presented as the mean \pm SD from three independent experiments. $*p < .05$, $**p < .01$, $***p < .001$



First, we assessed the generation of mitochondria by analyzing mtDNA copy number and immunofluorescence assay. The results showed that YBX1 deficiency didn't affect the mitochondrial number of brown adipocytes

(Figure 3A). Interestingly, the expression of transcription factors involved in mitochondrial biogenesis, including nuclear respiratory factor 1 (*Nrf1*) and transcription factor A, mitochondrial (*Tfam*), were downregulated

upon YBX1 knockdown (Figure 3B), suggesting that loss of YBX1 inhibited mitochondrial biogenesis. Thus, we presumed that YBX1 might promote mitochondria degradation. As expected, decreased MAP1LC3B-II:I ratio (autophagy marker) and increased SQSTM1/p62 (a protein specifically degraded in lysosomes) level were observed in YBX1-depleted cells (Figure 3C), indicating that there was attenuated autophagic flux. To further confirm whether YBX1 affects mitophagy, we examined the colocalization of mitochondria and autophagosome using MitoTracker and MAP1LC3B staining. Confocal images of YBX1-deficient brown adipocytes showed a significantly decreased number of red puncta and yellow signal (Figure 3D,E), indicating that alleviated mitophagy than control brown adipocytes. Accordingly, we observed less number of autophagosomes in YBX1-deficient cells using transmission electron microscopy (Figure 3F). The decreased mitochondrial biogenesis but equivalent mitochondrial content in YBX1-deficient cells suggests the defective mitochondrial clearance and deceleration of mitochondrial turnover, which would be due to impaired mitophagy in the absence of YBX1.

To validate whether YBX1 affects thermogenesis through mitophagy, we treated control and YBX1-overexpressing cells with or without mitophagy inhibitor. Mdivi-1 is a specific inhibitor of mitochondrial fission protein dynamin-related protein 1 (DRP1), which is now widely considered as a specific mitochondrial fission/mitophagy inhibitor.^{19,20} We found that Mdivi-1 treatment reversed the increased mRNA levels and protein abundance of thermogenic genes upon YBX1 overexpression (Figure 3G,H). Moreover, the upregulated thermogenic gene expression in YBX1-overexpressing cells could also be restored by mitophagosome formation inhibitor 3-methyladenine (3-MA)²¹ (Figure 3G,H). To determine the effect of YBX1 and mitophagy on thermogenesis, we used Seahorse Flux Analyzer to measure the OCR of cells. Importantly, YBX1 overexpression increased basal OCR and maximum respiratory capacity

in primary brown adipocytes, which could be alleviated upon Mdivi-1 and 3-MA treatments (Figure 3I). Together, these findings demonstrate that YBX1 facilitates the thermogenesis of brown fat cells through enhancing mitophagy.

3.4 | YBX1 enhances mitophagy via promoting mRNA stability of *Pink1* and *Prkn*

To further elucidate the underlying molecular mechanism of YBX1 in mitophagy regulation, we detected the expression of mitophagy-related genes upon YBX1 knockdown. We found that YBX1 deficiency dramatically decreased mRNA levels of *Pink1* and *Prkn*, two key mitophagy-related genes, while *Bnip3* and *Fundc1* were unchanged (Figure 4A). Consistently, the protein expression of PINK1 and PRKN were repressed upon YBX1 knockdown (Figure 4B). In contrast, YBX1 overexpression increased the mRNA and protein levels of *Pink1* and *Prkn* (Figure 4C,D), suggesting that YBX1 positively regulates PINK1/PRKN pathway. To test whether YBX1 influences thermogenesis through PINK1/PRKN pathway, we performed a rescue experiment and found that knockdown of PINK1 or PRKN could reverse the upregulated mRNA expression of *Ucp1* and *Ppargc1a* in YBX1-overexpressing cells (Figure 4E). Thus, YBX1 affects thermogenic gene expression by regulating PINK1 and PRKN expression.

Since YBX1 is a DNA/RNA binding protein, it is important to investigate the specific role of YBX1 in the modulation of *Pink1* and *Prkn* expression. We tested through detecting the cellular distribution of YBX1 in primary brown adipocytes and found that YBX1 protein was predominantly localized in the cytoplasm during adipogenesis (Figure 4F), suggesting that YBX1 mainly serves as a RBP in brown adipocytes, rather than a transcription factor. Using RBPDB database (<http://>

FIGURE 4 YBX1 positively regulates mitophagy through targeting and stabilizing *Pink1* and *Prkn* mRNAs. (A) qPCR analysis of mRNA expression of genes involved in mitophagy (*Pink1*, *Prkn*, *Bnip3*, and *Fundc1*) in differentiated brown preadipocytes treated with NC or *Ybx1* siRNA. (B) Western blot analysis of protein expression of PINK1 and PRKN in differentiated brown preadipocytes treated with NC or *Ybx1* siRNA. (C) qPCR analysis of mRNA expression of *Pink1* and *Prkn* in EGFP or YBX1-overexpressing brown adipocytes. (D) Western blot analysis of protein expression of PINK1 and PRKN in EGFP or YBX1-overexpressing brown adipocytes. (E) qPCR analysis of mRNA expression of *Ucp1*, *Ppargc1a*, *Pink1*, and *Prkn* in EGFP or YBX1-overexpressing cells transfected with or without *Pink1* or *Prkn* siRNA. ****p* < .001, Ad-YBX1 group compared to Ad-EGFP group. (F) Cellular distribution of YBX1 in differentiating brown adipocytes. (G) The analysis of potential YBX1-binding sites within *Pink1* and *Prkn* mRNA using the RBPDB database. (H) Western blot to confirm the immunoprecipitation of FLAG protein. (I) RNA immunoprecipitation-qPCR (RIP-qPCR) analysis of the interaction of *Pink1*, *Prkn*, *Ucp1*, and *Ppargc1a* mRNAs with FLAG in cells overexpressing EGFP or FLAG-tagged YBX1. *Ybx1* was used as the positive control, *Actb* was used as the negative control. (J) mRNA lifetimes of *Pink1* and *Prkn* in differentiated brown preadipocytes treated with NC or *Ybx1* siRNA. (K) mRNA lifetimes of *Bnip3*, *Ucp1*, and *Ppargc1a* in differentiated brown preadipocytes treated with NC or *Ybx1* siRNA. The data were presented as the mean \pm SD from three independent experiments. ***p* < .01, ****p* < .001

rbpdb.ccb.utoronto.ca/)²² to predict whether YBX1 binds to mitophagy-related mRNAs, the results showed that YBX1 may bind to *Pink1* and *Prkn* with multiple potential binding sites, but not *Bnip3* and *Fundc1* (Figure 4G).²³ To further confirm whether *Pink1* and *Prkn* transcripts were targets of YBX1 in mouse primary brown adipocytes and verify their exact binding sites, we infected the cells with YBX1-expressing adenovirus and performed RNA immunoprecipitation-qPCR (RIP-qPCR) with gene-specific primers. The FLAG-tagged YBX1 was successfully precipitated using FLAG beads (Figure 4H). A previous study reported that YBX1 could bind to its own mature mRNA, which was used as a positive control,^{24,25} while *Actb* was chosen as the negative control. The RIP-qPCR analysis identified that YBX1 directly bonds to the coding sequence (CDS) region of *Pink1* and *Prkn* mRNAs (Figure 4I), as the previous report that YBX1-to-RNA binding site mainly located in coding regions and 3'UTRs.²⁶ Of note, we found that YBX1 preferred to recognize *Pink1* at CDS of the range 1046–1051 and 1259–1264, and target *Prkn* at CDS of the range 244–249 (Figure 4I). In addition, we tested whether YBX1 directly targets mRNAs of thermogenic genes and confirmed that *Ucp1* and *Ppargc1a* were not direct targets of YBX1 (Figure 4I). Together, these results suggested that both *Pink1* and *Prkn* transcripts were targets of YBX1.

Numerous studies have implicated YBX1, as a multifunctional RBP, that regulates mRNA stability, decay, translation, and localization in mammals.^{14,27,28} The positive correlation between YBX1 expression and mRNA levels of *Pink1* and *Prkn* implied that YBX1 may stabilize their mRNAs. Indeed, we further validated that loss of YBX1 shortened the lifespan of *Pink1* and *Prkn* mRNAs (Figure 4J), whereas the *Bnip3* mRNA stability was unchanged (Figure 4K). These results indicated that YBX1 deficiency decreased protein expression of PINK1 and PRKN through directly binding and destabilizing their mRNAs. Taken together, these our findings demonstrate that YBX1 enhances mitophagy via promoting *Pink1* and *Prkn* mRNA stability.

3.5 | YBX1 is a key factor regulating energy expenditure and thermogenesis in vivo

To investigate the function of YBX1 in a thermogenic commitment under physiologic conditions in vivo, we specifically injected EGFP- or YBX1-expressing adenovirus into interscapular BAT of 8-week-old mice. After 1 week of virus injection, we first isolated the BAT to detect the overexpression efficiency. Immunofluorescence

image of BAT from mice infected with Ad-EGFP or Ad-YBX1 showed robust EGFP expression, indicating the success of virus infection (Figure 5A). Using qPCR and western blot analysis, we confirmed that YBX1 was overexpressed in BAT (Figure 5B,C). Compared with the control group, mice infected with Ad-YBX1 had higher core body temperature at room temperature (Figure 5D). Moreover, mice infected with Ad-YBX1 maintained body temperature against acute cold exposure more efficiently than mice infected with Ad-EGFP (Figure 5E). Immunofluorescence analysis also revealed facilitated UCP1 expression in BAT from mice infected with Ad-YBX1 when compared with the control group (Figure 5A). Furthermore, thermographic imaging of these mice showed that overexpression of YBX1 increased the surface temperature of BAT compared to the control group at room temperature (Figure 5F). There are even more significant differences between them under cold exposure conditions (Figure 5G). Consistent with this phenotype, YBX1 overexpression increased the mRNA and protein expression of thermogenic genes *Ucp1* and *Ppargc1a* in BAT (Figure 5H,I). These results suggest that YBX1 promotes energy expenditure and thermogenesis in vivo.

To confirm whether YBX1 influenced mitophagy in vivo, we detected the expression of mitophagy-related genes in BAT from mice infected with Ad-EGFP or Ad-YBX1. Compared with the control group, the MAP1LC3B-II:I ratio was increased in the YBX1-overexpressed group (Figure 5I). Furthermore, forced expression of YBX1 in BAT promoted the mRNA levels and protein abundance of *Pink1* and *Prkn* (Figure 5H,I). Collectively, these findings show that YBX1 enhances thermogenesis and PINK1/PRKN-mediated mitophagy in vivo.

4 | DISCUSSION

Cold shock proteins in bacteria are known to be involved in adaptation to low temperatures.^{15,29} Emerging evidence showed that CSD-containing proteins played critical roles in BAT thermogenesis.^{13,30} YBX family protein harbors an evolutionarily conserved CSD. Knockout of YBX2 impaired cold-induced brown fat activation in mice and brown adipogenesis.¹³ A recent study showed that YBX1 abundance was increased in subcutaneous WAT and BAT upon cold exposure in mice.¹⁶ Knockdown of YBX1 inhibited white adipocytes browning and impaired thermogenic potential partially through mediating histone demethylase JMJD1c at the transcriptional level. However, the post-transcriptional mechanism of YBX1 in brown thermogenesis regulation and its function in brown fat in vivo remains unknown. In this study, we found the expression of YBX1 in BAT from mice following cold exposure and β -adrenergic agonist

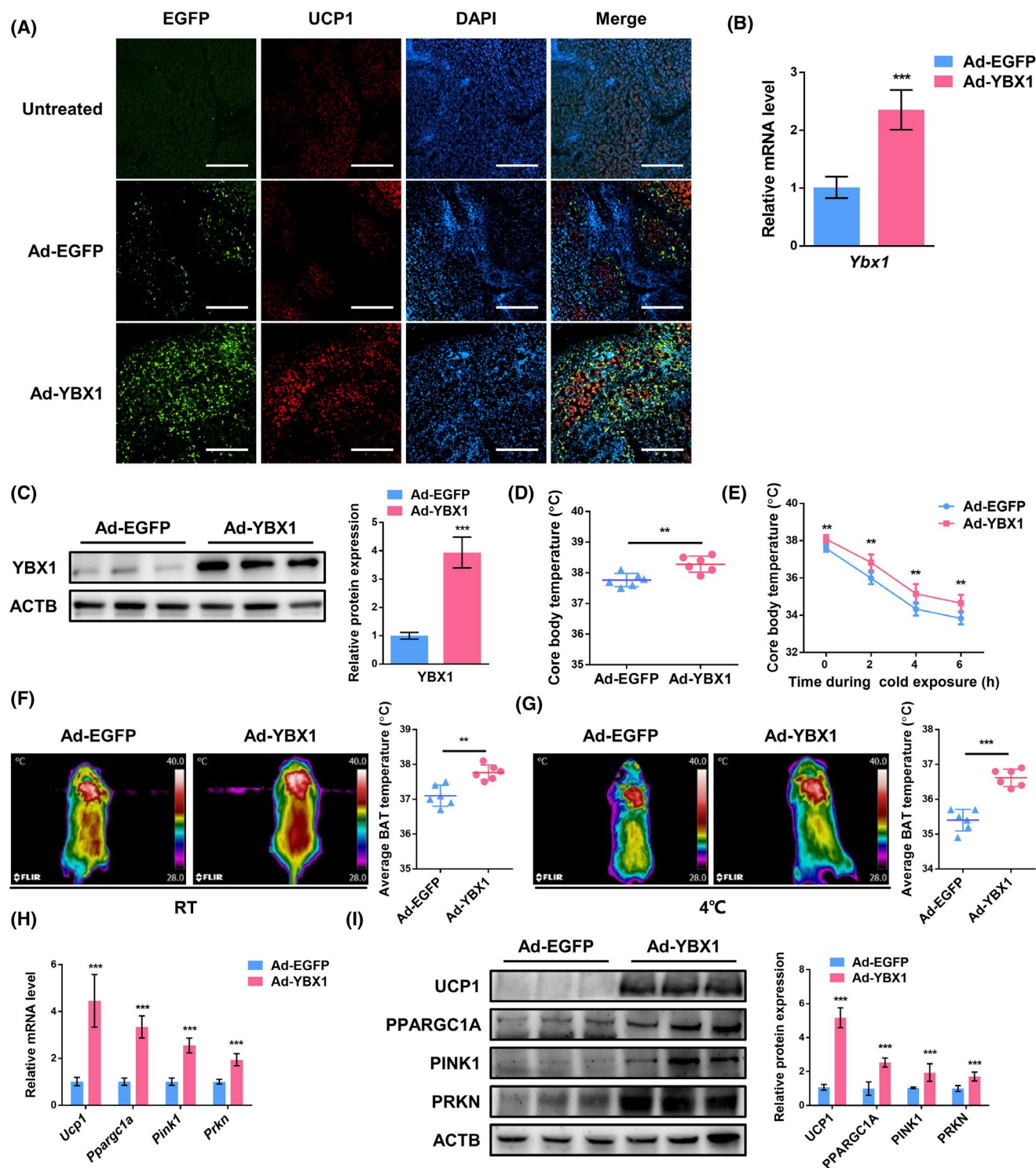


FIGURE 5 Overexpression of YBX1 in BAT enhances energy expenditure and thermogenesis in mice. (A) Immunofluorescence detection of EGFP and UCP1 in BAT from mice infected with Ad-EGFP or Ad-YBX1 for 1 week. Nuclei are stained with DAPI. Scale bar, 100 μ m. (B) qPCR analysis of mRNA expression of YBX1 in BAT from mice infected with Ad-EGFP or Ad-YBX1 for 1 week. (C) Western blot of analysis of protein expression of YBX1 in BAT from mice infected with Ad-EGFP or Ad-YBX1 for 1 week. (D) The rectal temperature of mice infected with Ad-EGFP or Ad-YBX1 at room temperature. (E) The rectal temperature of mice infected with Ad-EGFP or Ad-YBX1 during acute cold exposure and fasting for 6 h. (F) Thermal images and BAT temperatures of mice infected with Ad-EGFP or Ad-YBX1 at room temperature. (G) Thermal images and BAT temperatures of mice infected with Ad-EGFP or Ad-YBX1 at 4 $^{\circ}$ C for 6 h. (H) qPCR analysis of mRNA expression of *Ucp1*, *Ppargc1a*, *Pink1*, and *Prkn* in BAT from mice infected with Ad-EGFP or Ad-YBX1. (I) Western blot of analysis of protein expression of UCP1, PPARGC1A, MAP1LC3B, PINK1, and PRKN in BAT from mice infected with Ad-EGFP or Ad-YBX1. The data were presented as the mean \pm SD ($n = 6$). ** $p < .01$, *** $p < .001$.

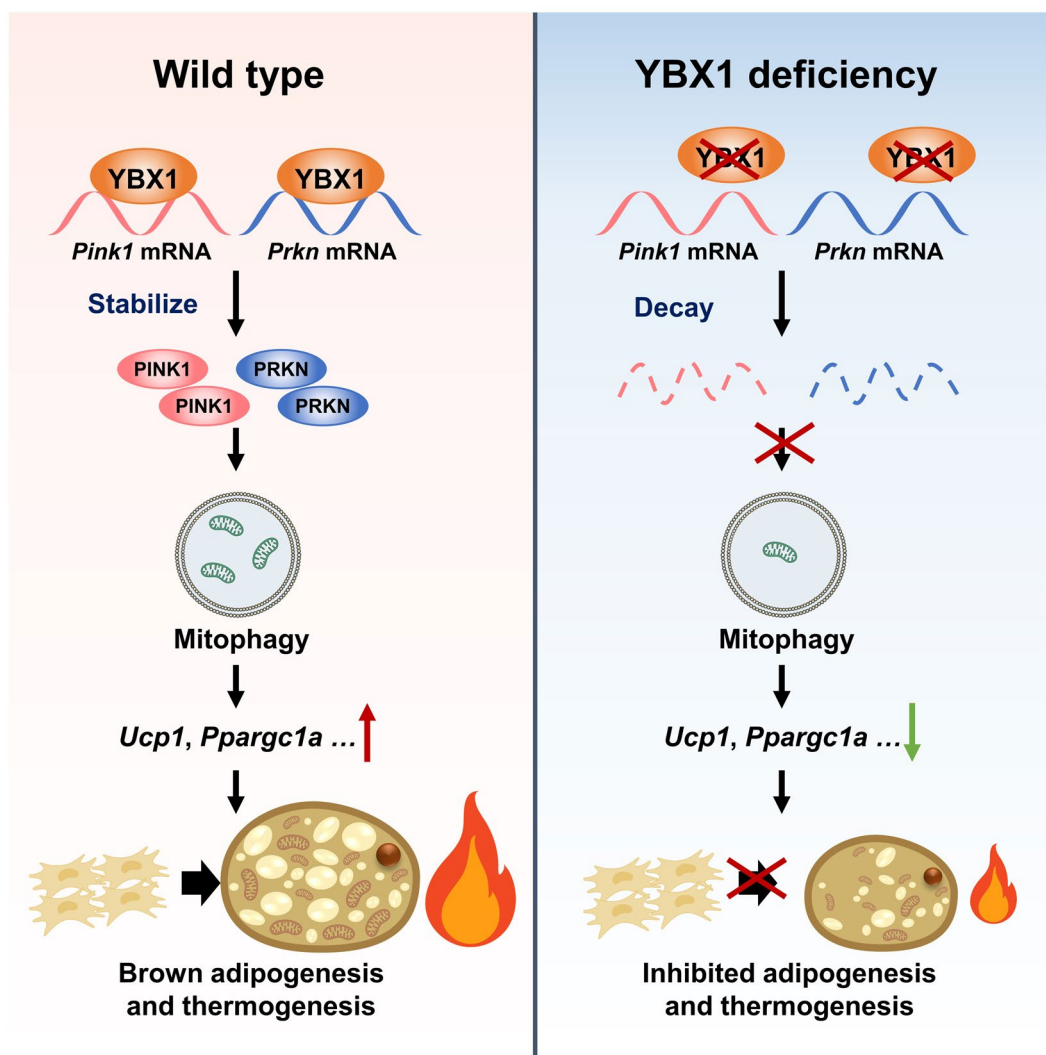


FIGURE 6 Proposed mechanism of YBX1 regulates brown adipocyte differentiation and thermogenic program through PINK1/PRKN-mediated mitophagy. In brown adipocytes, YBX1 specifically recognizes and binds to *Pink1* and *Prkn* mRNAs, protecting them from degradation, resulting in increased protein expression and enhanced mitophagy, thereby promoting adipogenesis and thermogenesis. YBX1 deficiency decreases mRNA stability and protein abundance of *Pink1* and *Prkn*, which in turn inhibits mitophagy and thermogenic gene expression, resulting in attenuated adipogenesis and thermogenesis

treatment, confirming the role of YBX1 in thermogenesis. At the cellular level, we showed that YBX1, as a RBP, positively regulated brown adipogenesis and thermogenesis by promoting mRNA stability of *Pink1* and *Prkn*. Furthermore, overexpression of YBX1 in BAT promoted energy expenditure and thermogenesis in mice. To better understand the explicit role of YBX1 in vivo, BAT-specific YBX1 knockout mice would be needed for further investigation.

Mitochondria plays key a role in energy metabolism, especially in thermogenic BAT. Accumulating evidence has suggested that mitophagy is required for BAT activation.^{6,31–33} The induction of mitophagy was observed in BAT of mice following cold exposure,⁷ indicating mitophagy is necessary for cold-induced thermogenesis. A recent study showed that mitophagy deficiency led to brown fat dysfunction and attenuated thermogenesis in mice.⁸

Lack of mitophagy receptor FUNDC1 in mice caused defective mitophagy and compromised mitochondrial quality, which resulted in declined energy expenditure and more severe obesity when fed a high-fat diet (HFD).⁹ Here, we showed that YBX1 promoted the thermogenic program of brown adipocytes through enhancing mitophagy. Mitophagy is important for mitochondrial remodeling and quality. We discovered a novel role for YBX1 as a positive mediator of mitophagy. YBX1 knockdown led to impaired mitophagy and decelerated mitochondrial turnover, which may partially contribute to the accumulation of dysfunctional mitochondria, thereby inhibiting thermogenesis. A previous study reported that YBX1 was known to localize to mitochondria,³⁴ and negatively regulate mitochondrial function in HeLa cells.³⁵ These findings suggest that YBX1 may play a cell type-specific

role in the regulation of mitochondrial function and mitophagy.

Previous studies showed that PINK1/PRKN-mediated mitophagy was of physiological importance to prevent metabolic disorders in various animal models.^{36,37} Global or BAT-specific deletion of *pink1* induced BAT dysfunction and obesity-prone type in mice.⁸ We found that YBX1 enhanced mitophagy by increasing the expression of PINK1 and PRKN, but not BNIP3 and FUNDC1. However, we cannot rule out that YBX1 may also regulate other mitophagy-related regulators or pathways, which needed to be tested by RIP couple with high throughput RNA-sequencing.

RNA-binding proteins play a critical role in modulating gene expression and signal pathways through determining RNA fate from synthesis to decay. Numerous studies have implicated YBX1 as a multifunctional DNA/RNA binding protein involved in transcriptional regulation, pre-mRNA splicing, mRNA stability, and translation.¹⁴ Given the cytoplasm localization of YBX1 in brown fat cells, we mainly focus on its effect on RNA. Our study further showed that YBX1 mediated *Pink1* and *Prkn* expression by promoting their mRNA stability. Similarly, YBX2 was found to control the mRNA stability of *Ppargc1a* to regulate brown fat thermogenesis.¹³ In HeLa cells, YBX1 was reported to impair mitochondrial function by suppressing translation of mRNAs coding for oxidative phosphorylation proteins.³⁵ YBX1 inhibits epidermal progenitor senescence by regulating the mRNA translation of a senescence-associated subset of cytokine.³⁸ The potential influence of YBX1 on translation in brown adipocytes is currently unknown and deserves further investigation. Additionally, YBX1 is a well-characterized transcription factor with the ability to translocate from the cytosol to the nucleus. We cannot exclude the possibility of YBX1 translocating into the nucleus and binding to DNA under specific circumstances, which will be further studied in the future.

In summary, our findings reveal that YBX1 plays a critical role in post-transcriptional regulation of brown adipocyte differentiation and thermogenic function through PINK1/PRKN-mediated mitophagy (Figure 6), which could be a promising target for therapy of obesity and the associated metabolic disease in the future. This study also expands our understanding of the underlying mechanisms of RNA-binding protein in regulating mitophagy and thermogenesis.

ACKNOWLEDGMENTS

This work was supported by the National Natural Science Foundation of China (31790411, 31972636), Project funded by the China Postdoctoral Science Foundation (2021M691073) and GuangDong Basic and Applied Basic Research Foundation (2021A1515111085).

DISCLOSURES

The authors declared no competing interests.

AUTHOR CONTRIBUTIONS

Designed the experiments: Ruifan Wu, Shuting Cao, and Qingyan Jiang. *Performed the experiments and analyzed the data:* Ruifan Wu, Shuting Cao, Fan Li, and Shengchun Feng. *Review the manuscript:* Canjun Zhu, Xiaotong Zhu, Lina Wang, Ping Gao, Gang Shu, Songbo Wang, and Qingyan Jiang. *Wrote the manuscript:* Ruifan Wu. All authors contributed to the article and approved the submitted version.

DATA AVAILABILITY STATEMENT

The data that support the findings of this study are available in the methods and supplementary material of this article.

ORCID

Ruifan Wu  <https://orcid.org/0000-0003-4917-5197>

Songbo Wang  <https://orcid.org/0000-0001-9190-9401>

REFERENCES

- Harms MJ, Ishibashi J, Wang W, et al. Prdm16 is required for the maintenance of brown adipocyte identity and function in adult mice. *Cell Metab.* 2014;19:593-604.
- Kajimura S, Spiegelman BM, Seale P. Brown and beige fat: physiological roles beyond heat generation. *Cell Metab.* 2015;22:546-559.
- Lowell BB, Spiegelman BM. Towards a molecular understanding of adaptive thermogenesis. *Nature.* 2000;404:652-660.
- Rosen ED, Spiegelman BM. What we talk about when we talk about fat. *Cell.* 2014;156:20-44.
- Liesa M, Shrihari OS. Mitochondrial dynamics in the regulation of nutrient utilization and energy expenditure. *Cell Metab.* 2013;17:491-506.
- Altshuler-Keylin S, Kajimura S. Mitochondrial homeostasis in adipose tissue remodeling. *Sci Signal.* 2017;10:eaai9248.
- Martinez-Lopez N, Garcia-Macia M, Sahu S, et al. Autophagy in the CNS and periphery coordinate lipophagy and lipolysis in the brown adipose tissue and liver. *Cell Metab.* 2016;23:113-127.
- Ko MS, Yun JY, Baek IJ, et al. Mitophagy deficiency increases NLRP3 to induce brown fat dysfunction in mice. *Autophagy.* 2021;17:1205-1221.
- Wu H, Wang Y, Li W, et al. Deficiency of mitophagy receptor FUNDC1 impairs mitochondrial quality and aggravates dietary-induced obesity and metabolic syndrome. *Autophagy.* 2019;15:1882-1898.
- Yau WW, Singh BK, Lesmana R, et al. Thyroid hormone (T3) stimulates brown adipose tissue activation via mitochondrial biogenesis and MTOR-mediated mitophagy. *Autophagy.* 2019;15:131-150.
- Inagaki T, Sakai J, Kajimura S. Transcriptional and epigenetic control of brown and beige adipose cell fate and function. *Nat Rev Mol Cell Biol.* 2017;18:527.
- Hentze MW, Castello A, Schwarzl T, Preiss T. A brave new world of RNA-binding proteins. *Nat Rev Mol Cell Biol.* 2018;19:327-341.
- Xu D, Xu S, Kyaw AMM, et al. RNA binding protein Ybx2 regulates RNA stability during cold-induced brown fat activation. *Diabetes.* 2017;66:2987-3000.

14. Lyabin DN, Eliseeva IA, Ovchinnikov LP. YB-1 protein: functions and regulation. *Wiley Interdiscip Rev RNA*. 2014;5:95-110.
15. Graumann PL, Marahiel MA. A superfamily of proteins that contain the cold-shock domain. *Trends Biochem Sci*. 1998;23:286-290.
16. Rabiee A, Plucinska K, Isidor MS, et al. White adipose remodeling during browning in mice involves YBX1 to drive thermogenic commitment. *Mol Metab*. 2021;44:101137.
17. Wang T, Xu YQ, Yuan YX, et al. Succinate induces skeletal muscle fiber remodeling via SUNC1 signaling. *EMBO Rep*. 2019;20:e47892.
18. Wang X, Lu Z, Gomez A, et al. N6-methyladenosine-dependent regulation of messenger RNA stability. *Nature*. 2014;505:117-120.
19. Mizumura K, Cloonan SM, Nakahira K, et al. Mitophagy-dependent necroptosis contributes to the pathogenesis of COPD. *J Clin Invest*. 2014;124:3987-4003.
20. Pi H, Xu S, Zhang L, et al. Dynamin 1-like-dependent mitochondrial fission initiates overactive mitophagy in the hepatotoxicity of cadmium. *Autophagy*. 2013;9:1780-1800.
21. Chen K, Dai H, Yuan J, et al. Optineurin-mediated mitophagy protects renal tubular epithelial cells against accelerated senescence in diabetic nephropathy. *Cell Death Dis*. 2018;9:105.
22. Cook KB, Kazan H, Zuberi K, Morris Q, Hughes TR. RBPDB: a database of RNA-binding specificities. *Nucleic Acids Res*. 2011;39:D301-D308.
23. Ray D, Kazan H, Chan ET, et al. Rapid and systematic analysis of the RNA recognition specificities of RNA-binding proteins. *Nat Biotechnol*. 2009;27:667-670.
24. Skabkina OV, Skabkin MA, Popova NV, Lyabin DN, Penalva LO, Ovchinnikov LP. Poly(A)-binding protein positively affects YB-1 mRNA translation through specific interaction with YB-1 mRNA. *J Biol Chem*. 2003;278:18191-18198.
25. Skabkina OV, Lyabin DN, Skabkin MA, Ovchinnikov LP. YB-1 autoregulates translation of its own mRNA at or prior to the step of 40S ribosomal subunit joining. *Mol Cell Biol*. 2005;25:3317-3323.
26. Wu SL, Fu X, Huang J, et al. Genome-wide analysis of YB-1-RNA interactions reveals a novel role of YB-1 in miRNA processing in glioblastoma multiforme. *Nucleic Acids Res*. 2015;43:8516-8528.
27. Evdokimova V, Ruzanov P, Imataka H, et al. The major mRNA-associated protein YB-1 is a potent 5' cap-dependent mRNA stabilizer. *EMBO J*. 2001;20:5491-5502.
28. Mordovkina D, Lyabin DN, Smolin EA, Sogorina EM, Ovchinnikov LP, Eliseeva I. Y-Box binding proteins in mRNP assembly, translation, and stability control. *Biomolecules*. 2020;10:591.
29. Lindquist JA, Mertens PR. Cold shock proteins: from cellular mechanisms to pathophysiology and disease. *Cell Commun Signal*. 2018;16:63.
30. Cheng H, Qi T, Zhang X, et al. Deficiency of heat shock protein A12A promotes browning of white adipose tissues in mice. *Biochim Biophys Acta Mol Basis Dis*. 2019;1865:1451-1459.
31. Kim D, Kim JH, Kang YH, et al. Suppression of brown adipocyte autophagy improves energy metabolism by regulating mitochondrial turnover. *Int J Mol Sci*. 2019;20:3520.
32. Lu Y, Fujioka H, Joshi D, et al. Mitophagy is required for brown adipose tissue mitochondrial homeostasis during cold challenge. *Sci Rep*. 2018;8:8251.
33. Ferhat M, Funai K, Boudina S. Autophagy in adipose tissue physiology and pathophysiology. *Antioxid Redox Sign*. 2019;31:487-501.
34. de Souza-Pinto NC, Mason PA, Hashiguchi K, et al. Novel DNA mismatch-repair activity involving YB-1 in human mitochondria. *DNA Repair*. 2009;8:704-719.
35. Matsumoto S, Uchiumi T, Tanamachi H, et al. Ribonucleoprotein Y-box-binding protein-1 regulates mitochondrial oxidative phosphorylation (OXPHOS) protein expression after serum stimulation through binding to OXPHOS mRNA. *Biochem J*. 2012;443:573-584.
36. Seillier M, Pouyet L, N'Guessan P, et al. Defects in mitophagy promote redox-driven metabolic syndrome in the absence of TP53INP1. *Embo Mol Med*. 2015;7:802-818.
37. Drew BG, Ribas V, Le JA, et al. HSP72Is a mitochondrial stress sensor critical for parkin action, oxidative metabolism, and insulin sensitivity in skeletal muscle. *Diabetes*. 2014;63:1488-1505.
38. Kwon E, Todorova K, Wang J, et al. The RNA-binding protein YBX1 regulates epidermal progenitors at a posttranscriptional level. *Nat Commun*. 2018;9:1734.

SUPPORTING INFORMATION

Additional supporting information may be found in the online version of the article at the publisher's website.

How to cite this article: Wu R, Cao S, Li F, et al. RNA-binding protein YBX1 promotes brown adipogenesis and thermogenesis via PINK1/PRKN-mediated mitophagy. *FASEB J*. 2022;36:e22219. doi:[10.1096/fj.202101810RR](https://doi.org/10.1096/fj.202101810RR)